

Xingjie Helen Li¹, Chi-Wang Shu² and Yang Yang³

Abstract

In this paper, we apply the local discontinuous Galerkin (LDG) method to 2D Keller-Segel (KS) chemotaxis model. We improve the results upon (Y. Epshteyn and A. Kurganov, SIAM Journal on Numerical Analysis, 47 (2008), 368-408) and give optimal rate of convergence under special finite element spaces. Moreover, to construct physically relevant numerical approximations, we develop a positivity-preserving limiter to the scheme, extending the idea in (Y. Zhang, X. Zhang and C.-W. Shu, Journal of Computational Physics, 229 (2010), 8918-8934). With this limiter, we can prove the L^1 -stability of the numerical scheme. Numerical experiments are performed to demonstrate the good performance of the positivity-preserving LDG scheme. Moreover, it is known that the chemotaxis model will yield blow-up solutions under certain initial conditions. We numerically demonstrate how to find the numerical blow-up time by using the L^2 -norm of the L^1 -stable numerical approximations.

Keywords: Local discontinuous Galerkin method, Keller-Segel chemotaxis model, positivity preserving, error estimate, Neumann boundary condition, blow-up, L^1 stability

¹Department of Mathematics and Statistics, University of North Carolina at Charlotte, Charlotte, NC 28223. E-mail: xli47@uncc.edu

²Division of Applied Mathematics, Brown University, Providence, RI 02912. E-mail: shu@dam.brown.edu. Research supported by ARO grant W911NF-15-1-0226 and NSF grant DMS-1418750.

³Department of Mathematical Sciences, Michigan Technological University, Houghton, MI 49931. E-mail: yyang7@mtu.edu

1 Introduction

In this paper, we study the Keller-Segel (KS) chemotaxis model in two space dimensions [33, 28] and focus on the following common formulation [3],

$$\begin{aligned} u_t - \operatorname{div}(\nabla u - \chi u \nabla v) &= 0, & x \in \Omega, t > 0, \\ v_t - \Delta v &= u - v, & x \in \Omega, t > 0, \end{aligned} \quad (1.1)$$

where Ω is assumed to be a convex, bounded and open set in \mathbb{R}^2 . Chemotaxis is the highly nonlinear terminology which indicates movements by cells in reaction to a chemical substance, where cells approach chemically favorable environments and avoid unpleasant ones. In (1.1), u and v denote the densities of cells and the chemical concentration, respectively. The chemotactic sensitivity function χ is assumed to be a positive constant. For simplicity, we take $\chi \equiv 1$. In addition, the initial conditions associated with (1.1) are given as

$$u(x, t = 0) = u^0(x), \quad v(x, t = 0) = v^0(x), \quad \text{for } x \in \Omega. \quad (1.2)$$

The boundary conditions are set to be homogeneous Neumann boundary condition

$$\nabla u \cdot \mathbf{n} = \nabla v \cdot \mathbf{n} = 0, \quad (1.3)$$

where \mathbf{n} is the outer normal of the boundary $\partial\Omega$. With this boundary condition, $\int_{\Omega} u \equiv \int_{\Omega} u^0$ is a constant during the time evolution and the system is thus isolated.

The existence and uniqueness of the weak solutions to (1.1) are not straightforward. In [16, 17], the initial densities u^0 and v^0 are assumed to be strictly positive and satisfy

$$u^0(x, y) \in L^2(\Omega), \quad u^0 \geq a^0 > 0 \text{ and } v^0(x, y) \in H_p^1(\Omega), \quad p > 2, \quad \forall (x, y) \in \Omega. \quad (1.4)$$

Furthermore, u^0 is assumed to hold a smallness condition [16], that is, there exists a constant $C_{\Omega}^{\text{GNS}} > 0$, such that

$$C_{\Omega}^{\text{GNS}} \chi \|u^0\|_{L^1(\Omega)} < 1,$$

where C_{Ω}^{GNS} denotes the best constant in the Gagliardo-Nirenberg-Sobolev inequality. Then for appropriate $T > 0$, there exists a couple of unique weak solution [17]

$$u \in C([0, T]; L^2(\Omega) \cap L^2(0, T; H^1(\Omega))), \quad v \in L^2(0, T; H^1(\Omega)). \quad (1.5)$$

The exact solutions of the KS chemotaxis model are always positive. Moreover, the model exhibits blow-up patterns with certain initial conditions [31, 24, 23, 17, 16]. Biologically, finite-time blow up for solutions is expected to describe chemotactic collapse, that is the tendency of cells to concentrate to form spora, which can be explained mathematically as concentration of $u(x, t)$ towards a Dirac mass in finite time [24, 31] in the sense of distribution. When the blow-up patterns occur, the density u of cells will strengthen in the neighborhood of isolated points, and these regions become sharper and eventually result in finite time point-wise blow-up. It was proved in [31] that blow-up never occurs in 1D space, whereas blow-up occurs within finite time in 2D and 3D cases. In 2D space, mathematical proofs for spherically symmetric solutions in a ball have been investigated in [23, 31]. When the initial mass is greater than certain threshold $\chi\|u^0\|_{L^1(\Omega)} > 8\pi$, then the exact solution will blow up at the center of the ball, and it is proved to be the only possible singularity. For nonsymmetric cases, if $4\pi < \chi\|u^0\|_{L^1(\Omega)} < 8\pi$ and the corresponding solution of (1.1) blows up at finite time, then the blow-up happens at the boundary of Ω [25, 26]. However, no such restriction in mass appears for the 3D case [23]. More theoretical works can be found in [17, 24, 23, 25].

It is difficult to construct numerical schemes for (1.1), and most of the previous works are for the following simplified system

$$\begin{aligned} u_t - \operatorname{div}(\nabla u - \chi u \nabla v) &= 0, & x \in \Omega, t > 0, \\ -\Delta v &= u - v, & x \in \Omega, t > 0, \end{aligned}$$

(See, for example, [41, 29, 16, 22] and the references therein). Recently, there are some significant works designed to solve (1.1) directly [32, 15, 37, 40]. In [32], the authors used the semigroup methods to obtain the stability and error estimates of the finite element methods. Later, In [37], the author constructed conservative upwind finite-element method to yield positive numerical approximations under some assumptions of the meshes. Subsequently, in [40], the authors constructed implicit second-order positivity preserving finite-volume schemes in three-dimensional space, and their technique requires solving a large linear system of equations coupling together all grid points at each stage of the two stage TR-BDF2

method when updating the diffusion terms at each time step. In [15], the authors applied the interior penalty discontinuous Galerkin (IPDG) method on rectangular meshes to obtain suboptimal rate of convergence, and the finite element space is assumed to be piecewise polynomials of degree $k \geq 2$. Other related works in this direction include [14, 12, 13] and the positivity-preserving property was demonstrated by numerical experiments only. Besides the above, in [36] the authors constructed positive numerical approximations by using the conservative upwind finite element method for the simplified system. Later in [2], the authors constructed a second order positivity-preserving scheme to a revised system by differentiating (1.1) with respect to x and y , hence the schemes were not designed to solve (1.1) directly. Subsequently, in [21], the author developed a composite particle-grid numerical method with adaptive time stepping to resolve and propagate singular solutions of (1.1). Recently, Zhang and Shu introduced positivity-preserving limiter to hyperbolic equations in [48, 49, 50]. Subsequently, the idea was extended to parabolic problems in [51]. In this paper, we will apply the positivity-preserving limiter introduced in [51] to construct second-order positivity-preserving local discontinuous Galerkin (LDG) schemes to obtain physically relevant numerical approximations. The method we plan to use preserves the positivity of the numerical solutions, and can be applied to unstructured meshes.

The DG method was first introduced in 1973 by Reed and Hill [35] in the framework of neutron linear transport. Subsequently, Cockburn et al. developed Runge-Kutta discontinuous Galerkin (RKDG) methods for hyperbolic conservation laws in a series of papers [9, 6, 8, 10]. In [11], Cockburn and Shu introduced the LDG method to solve the convection-diffusion equations. Their idea was motivated by Bassi and Rebay [1], where the compressible Navier-Stokes equations were successfully solved. Recently, the DG methods were applied to linear hyperbolic equations with δ -singularities [44] to obtain high-order approximations under suitable negative-order norms. Subsequently, the methods have also been applied to nonlinear hyperbolic equations with δ -singularities [45, 52]. Combined with special limiters, the schemes were proved to be L^1 stable [45, 34]. Recently, the idea has been extended to

parabolic equations with blow-up solutions by using the LDG method [20]. In this paper, we follow the same direction and employ the LDG method to capture the blow-up phenomenon. In the LDG method, we introduce auxiliary variables $\mathbf{p} = \nabla u$. Numerical experiments will be given to demonstrate the optimal rate of convergence. However, in this problem the approximations of \mathbf{p} is discontinuous across the cell interfaces and it is difficult to obtain error estimates if we analyze the convection and diffusion terms separately. To explain this point, let us consider the following hyperbolic equation

$$u_t + (a(x)u)_x = 0,$$

where $a(x)$ is discontinuous at $x = x_0$. In [18, 27], the authors studied such a problem and defined

$$Q = \frac{a(x_0 + b) - a(x_0)}{b}.$$

If Q is bounded from below for all b , then the solution exists, but may not be unique. If Q is bounded from above for all b , we can guarantee the uniqueness, but the solution may not exist. To bridge this gap, most of the previous works for similar problems are based on mixed finite element methods (see e.g. [29]). In this paper, we consider a new technique for error analysis following the idea in [42, 43]. Moreover, we also apply the positivity-preserving limiter to guarantee positivity of the numerical approximation. With this special technique, the L^1 norm of the numerical approximation is a constant during the time evolution due to the mass conservation. However, the L^2 norm might still be unbounded when blow-up patterns occur. We thus introduce a new idea to capture the numerical blow-up time based on the L^2 norm of the numerical approximations. To our best knowledge, this is the first paper studying the numerical blow-up time with a concrete theoretical background.

The organization of this paper is as follows. In Section 2, we construct the LDG scheme. In Section 3, we give the error estimates based on two different finite element spaces. In Section 4, we discuss the positivity-preserving technique, the foundation of limiters and high order time discretizations. Numerical experiments are given in Section 5. Finally, we will end in Section 6 with concluding remarks and remarks for future work.

2 The LDG scheme

In this section, we define the finite element spaces and proceed to construct the LDG scheme.

Let $\Omega_h = \{K\}$ be a quasi-uniform partition of the domain Ω with rectangular or triangular element K . Denote h_K be the diameter of element K , and $h = \max_K h_K$. We define the finite element space V_h^k as

$$V_h^k = \{z : z|_K \in P^k(K), \forall K \in \Omega_h\},$$

where $P^k(K)$ denotes the set of polynomials of degree up to k in cell K .

We choose $\boldsymbol{\beta}$ to be a fixed vector that is not parallel to any normals of element interfaces. Moreover, we denote Γ_h be the set of all element interfaces and $\Gamma_0 = \Gamma_h \setminus \partial\Omega$. Let $e \in \Gamma_0$ be an interior edge shared by elements K_ℓ and K_r , where $\boldsymbol{\beta} \cdot \mathbf{n}_\ell > 0$, and $\boldsymbol{\beta} \cdot \mathbf{n}_r < 0$, respectively, with \mathbf{n}_ℓ and \mathbf{n}_r being the outward normals of K_ℓ and K_r , respectively. For any $z \in V_h^k$, we define $z^- = z|_{\partial K_\ell}$ and $z^+ = z|_{\partial K_r}$, respectively. The jump is given as $[z] = z^+ - z^-$. Moreover, for $\mathbf{s} \in \mathbf{V}_h^k = V_h^k \times V_h^k$, we define \mathbf{s}^+ , \mathbf{s}^- and $[\mathbf{s}]$ analogously. Furthermore, we also denote $\boldsymbol{\nu}_e = \mathbf{n}_\ell$ to be the normal of e such that $\boldsymbol{\nu}_e \cdot \boldsymbol{\beta} > 0$. Similarly, we also define $\partial\Omega_- = \{e \in \partial\Omega | \boldsymbol{\beta} \cdot \mathbf{n} < 0, \mathbf{n} \text{ is the outer normal of } e\}$, and $\partial\Omega_+ = \partial\Omega \setminus \partial\Omega_-$.

To construct the LDG scheme, we introduce the auxiliary variables $\mathbf{p} = \nabla u$ and $\mathbf{r} = \nabla v$, then (1.1) can be written as

$$\begin{aligned} u_t &= -\nabla \cdot (\mathbf{r}u) + \nabla \cdot \mathbf{p}, \\ \mathbf{p} &= \nabla u, \\ v_t &= \nabla \cdot \mathbf{r} + u - v, \\ \mathbf{r} &= \nabla v. \end{aligned}$$

The LDG scheme is to find $u_h \in V_h^{k_1}$, $\mathbf{p}_h \in \mathbf{V}_h^{k_1}$, $v_h \in V_h^{k_2}$ and $\mathbf{r}_h \in \mathbf{V}_h^{k_2}$, such that for any test functions $w^u \in V_h^{k_1}$, $\mathbf{w}^p \in \mathbf{V}_h^{k_1}$, $w^v \in V_h^{k_2}$ and $\mathbf{w}^r \in \mathbf{V}_h^{k_2}$

$$(u_{ht}, w^u)_K = (\mathbf{r}_h u_h - \mathbf{p}_h, \nabla w^u)_K - \langle (\widehat{\mathbf{r}_h u_h} - \widehat{\mathbf{p}_h}) \cdot \mathbf{n}_K, w^u \rangle_{\partial K} \quad (2.1)$$

$$(\mathbf{p}_h, \mathbf{w}^p)_K = -(u_h, \nabla \cdot \mathbf{w}^p)_K + \langle \widehat{u}_h, \mathbf{w}^p \cdot \mathbf{n}_K \rangle_{\partial K}, \quad (2.2)$$

$$(v_{ht}, w^v)_K = -(r_h, \nabla w^v)_K + \langle \widehat{\mathbf{r}}_h \cdot \mathbf{n}_K, w^v \rangle_{\partial K} + (u_h - v_h, w^v)_K, \quad (2.3)$$

$$(\mathbf{r}_h, \mathbf{w}^r)_K = -(v_h, \nabla \cdot \mathbf{w}^r)_K + \langle \widehat{v}_h, \mathbf{w}^r \cdot \mathbf{n}_K \rangle_{\partial K}, \quad (2.4)$$

where $(u, v)_K = \int_K uv dx dy$, $(\mathbf{u}, \mathbf{v})_K = \int_K \mathbf{u} \cdot \mathbf{v} dx dy$ and $\langle u, v \rangle_{\partial K} = \int_{\partial K} uv ds$. We also denote \widehat{u}_h , \widehat{v}_h , $\widehat{\mathbf{p}}_h$, $\widehat{\mathbf{r}}_h$ and $\widehat{\mathbf{r}}_h \widehat{u}_h$ to be the numerical fluxes defined on $e \in \Gamma_h$. In this paper, we use the alternating fluxes for the diffusion terms. Due to the Neumann boundary condition (1.3), we take

1. For $e \in \Gamma_0$

$$(\widehat{u}_h, \widehat{\mathbf{p}}_h) = (u_h^+, \mathbf{p}_h^-), \quad (\widehat{v}_h, \widehat{\mathbf{r}}_h) = (v_h^+, \mathbf{r}_h^-), \quad (2.5)$$

2. For $e \in \partial\Omega_-$

$$(\widehat{u}_h, \widehat{\mathbf{p}}_h \cdot \mathbf{n}_K) = (u_h^+, 0), \quad (\widehat{v}_h, \widehat{\mathbf{r}}_h \cdot \mathbf{n}_K) = (v_h^+, 0), \quad (2.6)$$

3. For $e \in \partial\Omega_+$

$$(\widehat{u}_h, \widehat{\mathbf{p}}_h \cdot \mathbf{n}_K) = (u_h^-, 0), \quad (\widehat{v}_h, \widehat{\mathbf{r}}_h \cdot \mathbf{n}_K) = (v_h^-, 0), \quad (2.7)$$

For the convection term, we consider the Lax-Friedrichs flux: for any $e \in \Gamma_0$

$$\widehat{\mathbf{r}}_h \widehat{u}_h = \frac{1}{2} (\mathbf{r}_h^+ u_h^+ + \mathbf{r}_h^- u_h^- - \alpha \nu_e (u_h^+ - u_h^-)), \quad (2.8)$$

where $\alpha > 0$ is chosen by the positivity-preserving technique. Due to the mass conservation, if $e \in \partial\Omega$, we take

$$\widehat{\mathbf{r}}_h \widehat{u}_h \cdot \mathbf{n}_K = 0. \quad (2.9)$$

We also denote

$$(u, v) = \sum_{K \in \Omega_h} (u, v)_K, \quad (\mathbf{p}, \mathbf{r}) = \sum_{K \in \Omega_h} (\mathbf{p} \cdot \mathbf{r})_K,$$

then (2.1)-(2.4) can be written as

$$(u_{ht}, w^u) = \mathcal{L}^c(\mathbf{r}_h, u_h, w^u) - \mathcal{L}^d(\mathbf{p}_h, w^u), \quad (2.10)$$

$$(\mathbf{p}_h, \mathbf{w}^p) = -\mathcal{Q}(u_h, \mathbf{w}^p), \quad (2.11)$$

$$(v_{ht}, w^v) = -\mathcal{L}^d(\mathbf{r}_h, w^v) + (u_h - v_h, w^v), \quad (2.12)$$

$$(\mathbf{r}_h, \mathbf{w}^r) = -\mathcal{Q}(v_h, \mathbf{w}^r), \quad (2.13)$$

where

$$\mathcal{L}^c(\mathbf{r}, u, w) = (\mathbf{r}u, \nabla w) - \sum_{K \in \Omega_h} \langle \widehat{\mathbf{r}}_h u_h \cdot \mathbf{n}_K, w \rangle_{\partial K}, \quad (2.14)$$

$$\mathcal{L}^d(\mathbf{p}, w) = (\mathbf{p}, \nabla w) - \sum_{K \in \Omega_h} \langle \widehat{\mathbf{p}} \cdot \mathbf{n}_K, w \rangle_{\partial K}, \quad (2.15)$$

$$\mathcal{Q}(u, \mathbf{w}) = (u, \nabla \cdot \mathbf{w}) - \sum_{K \in \Omega_h} \langle u, \mathbf{w} \cdot \mathbf{n}_K \rangle_{\partial K} \quad (2.16)$$

It is easy to check the following identities by integration by parts on each cell: for any functions u and \mathbf{w} ,

$$\mathcal{L}^d(\mathbf{w}, u) + \mathcal{Q}(u, \mathbf{w}) = 0. \quad (2.17)$$

3 Error estimates

In this section, we analyze the error between the numerical and exact solutions. We first introduce the norms, construct the error equations and state the main theorem. Then we proceed to the proof. The whole procedure can be divided into several steps. We first construct the special projections that will be used in this section. Then we give an a priori error estimate and its verification. Finally, we will consider another finite element space and the corresponding error estimate. Let us define the norms first.

3.1 Norms

In this subsection, we define several norms that will be used throughout the paper.

Denote $\|u\|_{0,K}$ to be the standard L^2 norm of u in cell K . For any natural number ℓ , we consider the norm of the Sobolev space $H^\ell(K)$, defined by

$$\|u\|_{\ell,K} = \left\{ \sum_{0 \leq \alpha + \beta \leq \ell} \left\| \frac{\partial^{\alpha+\beta} u}{\partial x^\alpha \partial y^\beta} \right\|_{0,K}^2 \right\}^{\frac{1}{2}}.$$

Moreover, we define the norms on the whole computational domain as

$$\|u\|_\ell = \left(\sum_{K \in \Omega_h} \|u\|_{\ell,K}^2 \right)^{\frac{1}{2}}.$$

For convenience, if we consider the standard L^2 norm, then the corresponding subscript will be omitted.

Let Γ_K be the edges of K , and we define

$$\|u\|_{\Gamma_K}^2 = \int_{\partial K} u^2 ds.$$

We also define

$$\|u\|_{\Gamma_h}^2 = \sum_{K \in \Omega_h} \|u\|_{\Gamma_K}^2.$$

Moreover, we define the standard L^∞ norm of u in K as $\|u\|_{\infty,K}$, and define the L^∞ norm on the whole computational domain as

$$\|u\|_\infty = \max_{K \in \Omega_h} \|u\|_{\infty,K}.$$

Finally, we define similar norms for vector $\mathbf{u} = (u_1, u_2)^T$ as

$$\|\mathbf{u}\|_{\ell,K}^2 = \|u_1\|_{\ell,K}^2 + \|u_2\|_{\ell,K}^2, \quad \|\mathbf{u}\|_{\Gamma_K}^2 = \|u_1\|_{\Gamma_K}^2 + \|u_2\|_{\Gamma_K}^2, \quad \|\mathbf{u}\|_{\infty,K} = \max\{\|u_1\|_{\infty,K}, \|u_2\|_{\infty,K}\}.$$

Similarly, the norms on the whole computational domain are given as

$$\|\mathbf{u}\|_\ell^2 = \sum_{K \in \Omega_h} \|\mathbf{u}\|_{\ell,K}^2, \quad \|\mathbf{u}\|_{\Gamma_h}^2 = \sum_{K \in \Omega_h} \|\mathbf{u}\|_{\Gamma_K}^2, \quad \|\mathbf{u}\|_\infty = \max_{K \in \Omega_h} \|\mathbf{u}\|_{\infty,K}.$$

3.2 Error equations and the main theorem

In this subsection, we proceed to construct the error equations. Denote the error between the exact and numerical solutions to be

$$e_u = u - u_h, \quad \mathbf{e}_p = \mathbf{p} - \mathbf{p}_h, \quad e_v = v - v_h, \quad \mathbf{e}_r = \mathbf{r} - \mathbf{r}_h,$$

then we have the equations satisfied by the errors as

$$(e_{ut}, w^u) = \mathcal{L}^c(\mathbf{r}, u, w^u) - \mathcal{L}^c(\mathbf{r}_h, u_h, w^u) - \mathcal{L}^d(\mathbf{e}_p, w^u), \quad (3.1)$$

$$(\mathbf{e}_p, w^p) = -\mathcal{Q}(e_u, \mathbf{w}^p), \quad (3.2)$$

$$(e_{vt}, w^v) = -\mathcal{L}^d(\mathbf{e}_r, w^v) + (e_u - e_v, w^v), \quad (3.3)$$

$$(\mathbf{e}_r, \mathbf{w}^r) = -\mathcal{Q}(e_v, \mathbf{w}^r), \quad (3.4)$$

Now, we can state our main theorem.

Theorem 3.1. *Suppose $u, v \in H^{\min\{k_1, k_2\}+1}(\Omega)$, \mathbf{r} is uniformly bounded for $t \leq T$. The numerical approximations $u_h \in V_h^{k_1}$, $\mathbf{p}_h \in \mathbf{V}_h^{k_1}$, $v_h \in V_h^{k_2}$ and $\mathbf{r}_h \in \mathbf{V}_h^{k_2}$. The initial discretization is given as the standard L^2 -projection (3.14), and α is chosen to be a bounded constant independent of h . If we take $k_1 \geq 1$ and $k_2 \geq 2$, then there exists an H , given in Section 3.6, such that for any $h < H$, if the numerical approximations obtained from (2.10)-(2.13) exist for all $t \in [0, T]$, where T is the time that the smooth solution u and v of the KS system exist in $[0, T]$ then*

$$\|(u - u_h)(t)\| + \|(v - v_h)(t)\| \leq Ch^{\min\{k_1+1, k_2\}}, \forall t \in [0, T], \quad (3.5)$$

where the positive constant C does not depend on h .

3.3 Preliminaries and projections

In this subsection, we study the basic properties of the finite element space. Let us start with the classical inverse properties [4].

Lemma 3.1. *Assuming $\nu \in V_h^k$, there exists a positive constant C independent of h and ν such that*

$$h\|\nu\|_{\infty, K} + h^{1/2}\|\nu\|_{\Gamma_K} \leq C\|\nu\|_K.$$

In this paper, we consider several special projections. For any u and v , we define the elliptic projections \mathcal{P} from $H^1(\Omega) \times H^1(\Omega)$ into $V_h^{k_1} \times \mathbf{V}_h^{k_1} \times V_h^{k_2} \times \mathbf{V}_h^{k_2}$ by $\mathcal{P}(u, v) = (\mathcal{P}u, \mathcal{P}\mathbf{p}, \mathcal{P}v, \mathcal{P}\mathbf{r})$ such that for any $w^u \in V_h^{k_1}$, $\mathbf{w}^p \in \mathbf{V}_h^{k_1}$, $w^v \in V_h^{k_2}$ and $\mathbf{w}^r \in \mathbf{V}_h^{k_2}$

$$\mathcal{L}^d(\mathbf{p}, w^u) = \mathcal{L}^d(\mathcal{P}\mathbf{p}, w^u), \quad (3.6)$$

$$(\mathcal{P}\mathbf{p}, \mathbf{w}^p) = -\mathcal{Q}(\mathcal{P}u, \mathbf{w}^p) \quad (3.7)$$

$$\mathcal{L}^d(\mathbf{r}, w^v) = \mathcal{L}^d(\mathcal{P}\mathbf{r}, w^v), \quad (3.8)$$

$$(\mathcal{P}\mathbf{r}, \mathbf{w}^r) = -\mathcal{Q}(\mathcal{P}v, \mathbf{w}^r). \quad (3.9)$$

The existence of the elliptic projections will be given in the following lemma [5],

Lemma 3.2. *Suppose $\int_{\Omega} \mathcal{P}u dx dy = \int_{\Omega} u dx dy$ and $\int_{\Omega} \mathcal{P}v dx dy = \int_{\Omega} v dx dy$, then $\mathcal{P}u$, $\mathcal{P}\mathbf{p}$, $\mathcal{P}v$ and $\mathcal{P}\mathbf{r}$ are uniquely determined by (3.6)-(3.9). Moreover, we have the following estimates*

$$\|p - \mathcal{P}\mathbf{p}\| \leq Ch^{k_1}, \quad (3.10)$$

$$\|u - \mathcal{P}u\| \leq Ch^{k_1+1}, \quad (3.11)$$

$$\|r - \mathcal{P}\mathbf{r}\| \leq Ch^{k_2}, \quad (3.12)$$

$$\|v - \mathcal{P}v\| \leq Ch^{k_2+1}, \quad (3.13)$$

where C is independent of h .

In addition, we also define the standard L^2 projection P by

$$(Pu, v)_K = (u, v)_K, \quad \forall v \in P^k(K). \quad (3.14)$$

The L^2 projection satisfies the following property [4].

Lemma 3.3. *Suppose $u \in C^{k+1}(\Omega)$. Then there exists a positive constant C independent of h and u such that*

$$\|u - Pu\| + h\|u - Pu\|_{\infty} + h^{1/2}\|u - Pu\|_{\Gamma_h} \leq Ch^{k+1}\|u\|_{k+1}.$$

Let us finish this section by proving the following lemma.

Lemma 3.4. *Let $u \in C^{k+1}(\Omega)$ and $\Pi u \in V_h^k$. Suppose $\|u - \Pi u\| \leq Ch^{\kappa}$ for some positive constant C and $\kappa \leq k + 1$. Then*

$$h\|u - \Pi u\|_{\infty} + h^{1/2}\|u - \Pi u\|_{\Gamma_h} \leq Ch^{\kappa},$$

where the positive constant C does not depend on h .

Proof. Actually,

$$\begin{aligned}
& h\|u - \Pi u\|_\infty + h^{1/2}\|u - \Pi u\|_{\Gamma_h} \\
& \leq h\|Pu - \Pi u\|_\infty + h\|u - Pu\|_\infty + h^{1/2}\|Pu - \Pi u\|_{\Gamma_h} + h^{1/2}\|u - Pu\|_{\Gamma_h} \\
& \leq C\|Pu - \Pi u\| + Ch^{k+1} + C\|Pu - \Pi u\| + Ch^{k+1} \\
& \leq C\|u - \Pi u\| + C\|u - Pu\| + Ch^{k+1} \\
& \leq Ch^\kappa,
\end{aligned}$$

where the first and third steps follow from triangle inequality, the second step requires Lemma 3.1 and Lemma 3.3, and the last step we use Lemma 3.3. \square

3.4 A priori error estimate

In this subsection, we would like to make an a priori error estimate assumption that

$$\|u - u_h\| \leq h, \tag{3.15}$$

which further implies $\|u - u_h\|_\infty \leq C$ by Lemma 3.4. Moreover, if u is bounded, then $\|u_h\|_\infty \leq C$. Actually this a priori estimate assumption (3.15) holds for small enough h and this choice is heavily based on how large the constant C is in (3.5). Notice that the constant C depends on the exact solutions (u, v) of (1.1) as well as total time T , but is independent of h , as long as h is sufficiently small, say $h < H$. Then we can guarantee (3.15) holds for $\forall 0 \leq t \leq T$. Moreover, we will show that, if $h < H$, then the equality of (3.15) can not happen if $t < T$. However, we still need this estimate to obtain the boundedness of the numerical approximations. This assumption, which will be verified in Section 3.6, is used for the estimate of the convection terms. This idea has been used to obtain error estimates for nonlinear hyperbolic equations [46, 47, 30]. With this assumption, we can proceed to the main proof of the theorem.

3.5 Proof of Theorem 3.1

In this subsection, we give the proof of Theorem 3.1. We first assume the numerical approximations exist for all $0 < t < T$, and will verify this in Theorem 3.2. As the general treatment of the finite element methods, we divide the error as

$$\begin{aligned} e_u &= \eta_u - \xi_u, & \eta_u &= u - \mathcal{P}_u, & \xi_u &= u_h - \mathcal{P}_u, \\ \mathbf{e}_p &= \boldsymbol{\eta}_p - \boldsymbol{\xi}_p, & \boldsymbol{\eta}_p &= \mathbf{p} - \mathcal{P}_p, & \boldsymbol{\xi}_p &= \mathbf{p}_h - \mathcal{P}_p, \\ e_v &= \eta_v - \xi_v, & \eta_v &= v - \mathcal{P}_v, & \xi_v &= v_h - \mathcal{P}_v, \\ \mathbf{e}_r &= \boldsymbol{\eta}_r - \boldsymbol{\xi}_r, & \boldsymbol{\eta}_r &= \mathbf{r} - \mathcal{P}_r, & \boldsymbol{\xi}_r &= \mathbf{r}_h - \mathcal{P}_r. \end{aligned}$$

Clearly, $\xi_u, \boldsymbol{\xi}_p, \xi_v, \boldsymbol{\xi}_r$ are chosen from the desired finite element spaces, and following [42, 43], we have

Lemma 3.5.

$$\|\nabla \xi_u\|^2 + h^{-1} \|[\xi_u]\|_{\Gamma_h}^2 \leq C \|\boldsymbol{\xi}_p\|^2.$$

With the above lemma, we can proceed to the proof of Theorem 3.1.

Proof of Theorem 3.1. We take $w^u = \xi^u$, $\mathbf{w}^p = \boldsymbol{\xi}_p$, $w^v = \xi^v$ and $\mathbf{w}^r = \boldsymbol{\xi}_r$ in (3.1)-(3.4) to obtain

$$\frac{1}{2} \frac{d\|\xi_u\|^2}{dt} + \|\boldsymbol{\xi}_p\|^2 = T_1 - T_2, \quad (3.16)$$

$$\frac{1}{2} \frac{d\|\xi_v\|^2}{dt} + \|\boldsymbol{\xi}_r\|^2 = T_3, \quad (3.17)$$

where

$$T_1 = ((\eta_u)_t, \xi_u),$$

$$T_2 = (\mathbf{r}u - \mathbf{r}_h u_h, \nabla \xi_u) + \sum_{e \in \Gamma_0} \langle (\mathbf{r}u - \widehat{\mathbf{r}_h u_h}) \cdot \boldsymbol{\nu}_e, [\xi_u] \rangle_e,$$

$$T_3 = ((\eta_v)_t, \xi_v) - (\eta_u - \xi_u - \eta_v + \xi_v, \xi_v),$$

with

$$\langle u, v \rangle_e = \int_e uv ds$$

Now we give the estimates of T_i 's. By Cauchy-Schwarz inequality and Lemma 3.2

$$T_1 \leq \|(\eta_u)_t\| \|\xi_u\| \leq Ch^{k_1+1} \|\xi_u\|. \quad (3.18)$$

We rewrite T_2 into three terms.

$$\begin{aligned} T_2 &= (\mathbf{r}(u - u_h) + (\mathbf{r} - \mathbf{r}_h)u_h, \nabla \xi_u) + \sum_{e \in \Gamma_0} \langle (\mathbf{r}u - \widehat{\mathbf{r}}_h u_h) \cdot \boldsymbol{\nu}_e, [\xi_u] \rangle_e, \\ &= T_{21} + T_{22} + T_{23}, \end{aligned} \quad (3.19)$$

where

$$\begin{aligned} T_{21} &= (\mathbf{r}(u - u_h) + (\mathbf{r} - \mathbf{r}_h)u_h, \nabla \xi_u) \\ T_{22} &= \frac{1}{2} \sum_{e \in \Gamma_0} \langle (2\mathbf{r}u - \mathbf{r}_h^+ u_h^+ - \mathbf{r}_h^- u_h^-) \cdot \boldsymbol{\nu}_e, [\xi_u] \rangle_e \\ T_{23} &= \frac{1}{2} \sum_{e \in \Gamma_0} \langle \alpha[\eta_u - \xi_u], [\xi_u] \rangle_e, \end{aligned}$$

Using the fact that $\|\mathbf{r}\|_\infty \leq C$ and the a priori error estimate $\|u_h\|_\infty \leq C$, we have

$$\begin{aligned} T_{21} &\leq C (\|u - u_h\| + \|\mathbf{r} - \mathbf{r}_h\|) \|\nabla \xi_u\| \\ &\leq C (\|\eta_u\| + \|\xi_u\| + \|\boldsymbol{\eta}_r\| + \|\boldsymbol{\xi}_r\|) \|\boldsymbol{\xi}_p\| \\ &\leq C (h^{k_1+1} + \|\xi_u\| + h^{k_2} + \|\boldsymbol{\xi}_r\|) \|\boldsymbol{\xi}_p\|, \end{aligned} \quad (3.20)$$

where the first step is based on Cauchy-Schwarz inequality, the second step follows from Lemma 3.5 and triangle inequality, and in the last one we use Lemma 3.2. The estimate of T_{22} also requires the boundedness of \mathbf{r} and u_h ,

$$\begin{aligned} T_{22} &= \frac{1}{2} \sum_{e \in \Gamma_0} \langle (\mathbf{r}(u - u_h^+) + (\mathbf{r} - \mathbf{r}_h^+)u_h^+ + \mathbf{r}(u - u_h^-) + (\mathbf{r} - \mathbf{r}_h^-)u_h^-) \cdot \boldsymbol{\nu}_e, [\xi_u] \rangle_e \\ &\leq C (\|u - u_h\|_{\Gamma_h} + \|\mathbf{r} - \mathbf{r}_h\|_{\Gamma_h}) \|[\xi_u]\|_{\Gamma_h} \\ &\leq Ch^{1/2} (\|\eta_u\|_{\Gamma_h} + \|\xi_u\|_{\Gamma_h} + \|\boldsymbol{\eta}_r\|_{\Gamma_h} + \|\boldsymbol{\xi}_r\|_{\Gamma_h}) \|\boldsymbol{\xi}_p\| \\ &\leq C (h^{k_1+1} + \|\xi_u\| + h^{k_2} + \|\boldsymbol{\xi}_r\|) \|\boldsymbol{\xi}_p\|. \end{aligned} \quad (3.21)$$

Here in the second step we use Cauchy-Schwarz inequality, the third step follows from triangle inequality and Lemma 3.5, the last one requires Lemma 3.4 and Lemma 3.2. Now we proceed to the estimate of T_{23} ,

$$T_{23} \leq C (\|[\eta_u]\|_{\Gamma_h} + \|[\xi_u]\|_{\Gamma_h}) \|[\xi_u]\|_{\Gamma_h}$$

$$\begin{aligned}
&\leq Ch^{1/2}(\|[\eta_u]\|_{\Gamma_h} + \|[\xi_u]\|_{\Gamma_h}) \|\xi_p\| \\
&\leq C(h^{k_1+1} + \|\xi_u\|) \|\xi_p\|,
\end{aligned} \tag{3.22}$$

where the first step follows from Cauchy-Schwarz inequality, the second step is based on Lemma 3.5, the third one requires Lemma 3.4 and Lemma 3.2. Plug (3.20), (3.21) and (3.22) into (3.19) to obtain

$$T_2 \leq (Ch^{k_1+1} + Ch^{k_2} + C\|\xi_u\| + C\|\xi_r\|) \|\xi_p\|. \tag{3.23}$$

The estimate of T_3 is simple, we only use Cauchy-Schwarz inequality and Lemma 3.2,

$$\begin{aligned}
T_3 &\leq (\|(\eta_v)_t\| + \|\eta_u\| + \|\xi_u\| + \|\eta_v\| + \|\xi_v\|) \|\xi_v\| \\
&\leq C(h^{\min(k_1, k_2)+1} + \|\xi_u\| + \|\xi_v\|) \|\xi_v\|
\end{aligned} \tag{3.24}$$

Plug (3.18) and (3.23) into (3.16) to obtain

$$\begin{aligned}
\frac{1}{2} \frac{d\|\xi_u\|^2}{dt} + \|\xi_p\|^2 &\leq Ch^{k_1+1}\|\xi_u\| + C(h^{\min(k_1+1, k_2)} + \|\xi_u\|)\|\xi_p\| + C\|\xi_r\|\|\xi_p\| \\
&\leq C(h^{2\min(k_1+1, k_2)} + \|\xi_u\|^2 + \|\xi_r\|^2) + \|\xi_p\|^2,
\end{aligned}$$

which further implies

$$\frac{1}{2} \frac{d\|\xi_u\|^2}{dt} \leq C(h^{2\min(k_1+1, k_2)} + \|\xi_u\|^2 + \|\xi_r\|^2). \tag{3.25}$$

Moreover, plug (3.24) into (3.17) to yield

$$\frac{1}{2} \frac{d\|\xi_v\|^2}{dt} + \|\xi_r\|^2 \leq C(h^{\min(k_1, k_2)+1} + \|\xi_u\| + \|\xi_v\|) \|\xi_v\|. \tag{3.26}$$

Combining (3.25) and (3.26), we can find a constant γ such that

$$\begin{aligned}
&\frac{1}{2} \frac{d\|\xi_u\|^2}{dt} + \gamma \left(\frac{1}{2} \frac{d\|\xi_v\|^2}{dt} + \|\xi_r\|^2 \right) \\
&\leq C(h^{2\min(k_1+1, k_2)} + \|\xi_u\|^2 + \|\xi_r\|^2) + \gamma C(h^{\min(k_1, k_2)+1} + \|\xi_u\| + \|\xi_v\|) \|\xi_v\|
\end{aligned}$$

Take γ to be sufficiently large, we have

$$\frac{d\|\xi_u\|^2}{dt} + \gamma \frac{d\|\xi_v\|^2}{dt} \leq Ch^{2\min(k_1+1, k_2)} + C\|\xi_u\|^2 + C\|\xi_v\|^2.$$

Therefore, by the Gronwall's inequality and use L^2 -projection as the initial discretization,

$$\|\xi_u\|^2 + \|\xi_v\|^2 \leq Ch^{2\min(k_1+1, k_2)},$$

which further yield

$$\|u - u_h\| + \|v - v_h\| \leq Ch^{\min(k_1+1, k_2)}$$

by Lemma 3.2.

3.6 Verification of the a priori error estimate

In this section, we proceed to verify the a priori error estimate assumption (3.15). Notice that, (3.15) is true at $t = 0$. Suppose (3.15) fails before T , then let us denote $t^* = \inf\{t \mid \|(u - u_h)(t)\| > h\}$ and we have $0 < t^* < T$. Since $(u - u_h)(t)$ is a continuous function of the time variable t , at t^* we have $h = \|(u - u_h)(t^*)\|$. On the other hand, (3.15) holds for $0 \leq t \leq t^*$, thus from Theorem 3.1, we have $\|(u - u_h)(t^*)\| \leq Ch^{\min(k_1+1, k_2)}$, which is a contradiction if $k_1 \geq 1$, $k_2 \geq 2$ and h is smaller than $H = \frac{1}{2C}$. Therefore, we have $\|(u - u_h)(t)\| \leq h$ for $\forall 0 \leq t \leq T$. Now we have completed the verification of (3.15) and hence have finished the whole proof.

3.7 Existence of the numerical solutions

In this subsection, we proceed to prove the existence of the numerical approximations obtained from (2.10)-(2.13).

For a fixed mesh with $h < H$, we denote the ODE system (2.10)-(2.13) as $\frac{d}{dt}u_h = L^u(u_h, v_h)$ and $\frac{d}{dt}v_h = L^v(u_h, v_h)$, where u_h and v_h are the numerical approximations. Let T be the largest time such that u, v are smooth and \mathbf{p}, \mathbf{r} are bounded for any $t \in [0, T]$. Denote

$$T_h = \sup\{t_h : 0 < t_h \leq T, C^1 \text{ solution } (u_h(t), v_h(t)) \text{ exists in } 0 \leq t \leq t_h\}.$$

Then based on Theorem 3.1,

$$\|(u - u_h)(t)\| + \|(v - v_h)(t)\| \leq Ch^{\min\{k_1+1, k_2\}} \leq Ch^2, \quad \forall t \in [0, T_h], \quad (3.27)$$

with C independent of T_h and h . Take $\mathbf{w}^p = \boldsymbol{\xi}_p$ and $\mathbf{w}^r = \boldsymbol{\xi}_r$ in (3.2) and (3.4), respectively, we can easily obtain

$$\|(\mathbf{p} - \mathbf{p}_h)(t)\| + \|(\mathbf{r} - \mathbf{r}_h)(t)\| \leq Ch, \quad \forall t \in [0, T_h], \quad (3.28)$$

by Lemma 3.1. We will prove by contradiction and assume $T_h < T$, then there are two possibilities.

(1) The numerical solutions u_h and v_h exist at $t = T_h$. Then by the local existence of the ODE system, we can find some t_h such that u_h and v_h exist for $0 \leq t \leq T_h + t_h$, which is a contradiction.

(2) The numerical solution u_h does not exist at $t = T_h$ (The case for v_h should be exactly the same). Denote the local orthonormal polynomial basis in K to be L_1, L_2, \dots, L_ℓ with $\ell = \frac{k(k+1)}{2}$, then u_h can be written as $u_h(x, y, t) = \sum_{i=1}^{\ell} a_i(t) L_i(x, y)$. Therefore, we only need to show $a_i(t)$ exists at $t = T_h$ for any $i = 1, \dots, \ell$. Take $w^u = L_i$ in (2.10), we have $\forall t < T_h$,

$$\begin{aligned} \frac{d}{dt} a_i(t) &= \mathcal{L}^c(\mathbf{r}_h, u_h, L_i) - \mathcal{L}^d(\mathbf{p}_h, L_i) \\ &\leq Ch^{-1} \|\mathbf{r}_h\| \|u_h\|_{\infty} + Ch^{-1} \|\mathbf{p}_h\| \\ &\leq Ch^{-1} (\|u_h - u\|_{\infty} + \|u\|_{\infty}) \\ &\leq Ch^{-1}, \end{aligned}$$

where the second step follows from the inverse inequality (3.1), the third one is based (3.28) and the boundedness of \mathbf{p} and \mathbf{r} , in the last step we use (3.27) and Lemma 3.4. Choose $\tau < T_h$, since

$$a_i(t) = a_i(\tau) + \int_{\tau}^t a_i' dt, \quad \forall t \in [\tau, T_h],$$

$\{a_i(t_n)\}$ is Cauchy for any sequence $t_n \rightarrow T_h$. This implies $\lim_{t \rightarrow T_h} a_i(t)$ exists, defined as $a_i(T_h)$. So $a_i(t)$ has a continuous extension to $[0, T_h]$ such that

$$a_i(t) = a_i(\tau) + \int_{\tau}^t a_i' dt, \quad \forall t \in [\tau, T_h],$$

This is another contradiction since we have assumed the numerical solution u_h does not exist at $t = T_h$.

Finally, we have the following existence result

Theorem 3.2. *Suppose the assumptions in Theorem 3.1 hold true, then the numerical approximations exist in the interval $[0, T]$, where T is the time such that the exact solutions are bounded and smooth.*

3.8 Q^k polynomials

In this section, we consider rectangular meshes and give the error estimates under another finite element space. If not otherwise stated, we follow the same notations used before. We consider the computational domain to be $\Omega = [0, 1] \times [0, 1]$ and the fixed vector β is taken as $(1, 1)$. Let $0 = x_{\frac{1}{2}} < \dots < x_{N_x + \frac{1}{2}} = 1$ and $0 = y_{\frac{1}{2}} < \dots < y_{N_y + \frac{1}{2}} = 1$ be the grid points in the x and y directions. Let $K_{ij} = (x_{i-\frac{1}{2}}, x_{i+\frac{1}{2}}) \times (y_{j-\frac{1}{2}}, y_{j+\frac{1}{2}})$, $i = 1, \dots, N_x, j = 1, \dots, N_y$, be a partition of Ω , and the mesh sizes in the x and y directions are given as $\Delta x_i = x_{i+\frac{1}{2}} - x_{i-\frac{1}{2}}$ and $\Delta y_j = y_{j+\frac{1}{2}} - y_{j-\frac{1}{2}}$, respectively. For simplicity, we assume uniform meshes and denote $h = \Delta x_i = \Delta y_j$. However, this assumption is not essential in the proof. Moreover, we also denote $I_i = [x_{i-\frac{1}{2}}, x_{i+\frac{1}{2}}]$ and $J_j = [y_{j-\frac{1}{2}}, y_{j+\frac{1}{2}}]$ to be the cells in x and y directions. The finite element space W_h^k is defined as

$$W_h^k = \left\{ z : z|_{K_{ij}} \in Q^k(K_{ij}) \right\},$$

where $Q^k(K_{ij})$ denotes the set of tensor product polynomials of degree up to k in cell K_{ij} . In this section, we will take $v_h \in W_h^k$, $\mathbf{r}_h \in \mathbf{W}_h^k = W_h^k \times W_h^k$ and $u_h \in V_h^k$, $\mathbf{p}_h \in \mathbf{V}_h^k$ to obtain optimal error estimate. We first define several special projections. We define P_+ into W_h^k which is, for each cell K_{ij} ,

$$\begin{aligned} (P_+u - u, v)_{K_{ij}} &= 0, \quad \forall v \in Q^{k-1}(K_{ij}), \quad \int_{J_j} (P_+u - u)(x_{i-\frac{1}{2}}, y)v(y)dy = 0, \quad \forall v \in P^{k-1}(J_j), \\ (P_+u - u)(x_{i-\frac{1}{2}}, y_{j-\frac{1}{2}}) &= 0, \quad \int_{I_i} (P_+u - u)(x, y_{j-\frac{1}{2}})v(x)dx = 0, \quad \forall v \in P^{k-1}(I_i). \end{aligned} \quad (3.29)$$

Moreover, we also define Π_k^x and Π_k^y into W_h^k which are, for each cell K_{ij} ,

$$\begin{aligned} (\Pi_k^x u - u, v_x)_{K_{ij}} &= 0, \quad \forall v \in Q^k(K_{ij}), \quad \int_{J_j} (\Pi_k^x u - u)(x_{i+\frac{1}{2}}, y)v(y)dy = 0, \quad \forall v \in P^k(J_j), \\ (\Pi_k^y u - u, v_y)_{K_{ij}} &= 0, \quad \forall v \in Q^k(K_{ij}), \quad \int_{I_i} (\Pi_k^y u - u)(x, y_{j+\frac{1}{2}})v(x)dx = 0, \quad \forall v \in P^k(I_i). \end{aligned} \quad (3.30)$$

Further more, we define a two-dimensional projection $\mathbf{\Pi}_k = \Pi_k^x \otimes \Pi_k^y$. Following the same analysis before, we define

$$\eta_v = v - P_+ v, \quad \boldsymbol{\eta}_r = \mathbf{r} - \mathbf{\Pi}_k \mathbf{r},$$

and

$$\xi_v = v_h - P_+ v, \quad \boldsymbol{\xi}_r = \mathbf{r}_h - \mathbf{\Pi}_k \mathbf{r}.$$

Similar to Lemma 3.5, we would like to introduce the following one without proof.

Lemma 3.6. *Suppose ξ_v and $\boldsymbol{\xi}_r$ are defined above, we have*

$$\|\nabla \xi_v\| \leq C \|\boldsymbol{\xi}_r\|, \quad h^{-1} \|\xi_v\|_{\Gamma_h}^2 \leq C \|\boldsymbol{\xi}_r\|^2.$$

Moreover, we will use the following lemma [4]

Lemma 3.7. *Suppose v is sufficiently smooth, then we have*

$$\|\eta_v\| + h^{1/2} \|\eta_v\|_{\Gamma_h} \leq Ch^{k+1}, \quad (3.31)$$

$$\|\boldsymbol{\eta}_r\| + h^{1/2} \|\boldsymbol{\eta}_r\|_{\Gamma_h} \leq Ch^{k+1}, \quad (3.32)$$

Finally, we also need the superconvergence property of the bilinear form Q given in (2.16) [7].

Lemma 3.8. *For any $\mathbf{w} \in \mathbf{W}_h^k$, we have*

$$|Q(\eta_u, \mathbf{w})| \leq Ch^{k+1} \|u\|_{k+2} \|\mathbf{w}\|.$$

Now we can state the main theorem.

Theorem 3.3. *Suppose the exact solutions u, v are smooth and the derivatives r, s are uniformly bounded. The LDG scheme is defined as (2.1)-(2.4) with $u_h \in V_h^k$, $\mathbf{p}_h \in \mathbf{V}_h^k$, $v_h \in W_h^k$ and $\mathbf{r}_h \in \mathbf{W}_h^k$ for $k \geq 1$. Moreover, the initial discretization is also given as the L^2 -projection. Then we have*

$$\|u - u_h\| + \|v - v_h\| \leq Ch^{k+1}.$$

Proof. In the proof, we skip the a priori error estimate (3.15), its verification in Section 3.6 as well as most of the derivation steps, since they can be obtained from Section 3.5 with some minor changes. We take $w^u = \xi_u$, $\mathbf{w}^p = \boldsymbol{\xi}_p$, $w^v = \xi_v$ and $\mathbf{w}^r = \boldsymbol{\xi}_r$ in (3.1)-(3.4) to obtain

$$\frac{1}{2} \frac{d\|\xi_u\|^2}{dt} + \|\boldsymbol{\xi}_p\|^2 = T_1 - T_2, \quad (3.33)$$

$$\frac{1}{2} \frac{d\|\xi_v\|^2}{dt} + \|\boldsymbol{\xi}_r\|^2 = T_3 + T_4, \quad (3.34)$$

where

$$T_1 = ((\eta_u)_t, \xi_u),$$

$$T_2 = (\mathbf{r}u - \mathbf{r}_h u_h, (\xi_u)_x) + \sum_{e \in \Gamma_0} \langle (\mathbf{r}u - \widehat{\mathbf{r}_h u_h}) \cdot \boldsymbol{\nu}_e, [\xi_u] \rangle_e,$$

$$T_3 = ((\eta_v)_t, \xi_v) - (\eta_u - \xi_u - \eta_v + \xi_v, \xi_v),$$

$$T_4 = \mathcal{Q}(\eta_v, \boldsymbol{\xi}_r)$$

Following the analyses in Section 3.5, we obtain the estimates of T_i 's.

$$T_1 \leq Ch^{k+1} \|\xi_u\|. \quad (3.35)$$

$$T_2 \leq C(h^{k+1} + \|\xi_u\| + \|\boldsymbol{\xi}_r\|) \|\boldsymbol{\xi}_p\| \quad (3.36)$$

$$T_3 \leq C(h^{k+1} + \|\xi_u\| + \|\xi_v\|) \|\xi_v\| \quad (3.37)$$

Finally, the estimate of T_4 follows from Lemma 3.8 directly,

$$T_4 \leq Ch^{k+1} \|\boldsymbol{\xi}_r\|. \quad (3.38)$$

Plug (3.35) and (3.36) into (3.33) to obtain

$$\begin{aligned} \frac{1}{2} \frac{d\|\xi_u\|^2}{dt} + \|\xi_p\|^2 &\leq Ch^{k+1}\|\xi_u\| + C(h^{k+1} + \|\xi_u\|)\|\xi_p\| + C\|\xi_r\|\|\xi_p\| \\ &\leq C(h^{2k+2} + \|\xi_u\|^2 + \|\xi_r\|^2) + \|\xi_p\|^2, \end{aligned}$$

which further implies

$$\frac{1}{2} \frac{d\|\xi_u\|^2}{dt} \leq C(h^{2k+2} + \|\xi_u\|^2 + \|\xi_r\|^2). \quad (3.39)$$

Moreover, plug (3.37) and (3.38) into (3.34) to yield

$$\begin{aligned} \frac{1}{2} \frac{d\|\xi_v\|^2}{dt} + \|\xi_r\|^2 &\leq C(h^{k+1} + \|\xi_u\| + \|\xi_v\|)\|\xi_v\| + Ch^{k+1}\|\xi_r\| \\ &\leq C(h^{k+1} + \|\xi_u\| + \|\xi_v\|)\|\xi_v\| + Ch^{2k+2} + \frac{1}{2}\|\xi_r\|^2, \end{aligned}$$

which further implies

$$\frac{d\|\xi_v\|^2}{dt} + \|\xi_r\|^2 \leq C(h^{2k+2} + \|\xi_u\|^2 + \|\xi_v\|^2) \quad (3.40)$$

Combining (3.39) and (3.40), we can find a constant γ such that

$$\begin{aligned} &\frac{d\|\xi_u\|^2}{dt} + \gamma \left(\frac{d\|\xi_v\|^2}{dt} + \|\xi_r\|^2 \right) \\ &\leq C(h^{2k+2} + \|\xi_u\|^2 + \|\xi_r\|^2) + \gamma C(h^{2k+2} + \|\xi_u\|^2 + \|\xi_v\|^2) \end{aligned}$$

Take γ to be sufficiently large, then

$$\frac{d\|\xi_u\|^2}{dt} + \gamma \frac{d\|\xi_v\|^2}{dt} \leq Ch^{2k+2} + C\|\xi_u\|^2 + C\|\xi_v\|^2.$$

Therefore, by the Gronwall's inequality and L^2 initial discretization

$$\|\xi_u\|^2 + \|\xi_v\|^2 \leq Ch^{2k+2},$$

which further yield

$$\|u - u_h\| + \|v - v_h\| \leq Ch^{k+1}$$

by Lemma 3.2 and Lemma 3.7. □

4 Positivity preserving property

In this subsection, we apply the positivity-preserving technique to construct positive numerical approximations. In [51], the authors have studied the positivity-preserving technique for convection-diffusion equations on triangular meshes. Therefore, in this paper, we consider rectangular meshes only. If not otherwise stated, we follow the same notations defined in Section 3.8. Following the idea in [51], we restrict ourselves to the P^1 -LDG formulation. For simplicity, we consider Euler forward time discretization and the time step is Δt . Moreover, in this section, we also consider uniform meshes only, and denote the mesh sizes in the x and y directions as Δx and Δy , respectively. However, this assumption is not essential. Assume the numerical solutions at time level n are positive: $u_h^n > 0$, $v_h^n > 0$. Then we will construct positive numerical approximations at time level $n+1$. To do so, we will firstly prove that the cell average at time level $n+1$ is positive. Next, we can use a simple limiter to modify the DG polynomial and make it to be positive without changing its cell average. In this section, we denote $\mathbf{p} = (p, q)$ and $\mathbf{r} = (r, s)$. For simplicity, we use o to represent the exact solutions of the six variables u, p, q, v, r, s and o_h for the corresponding numerical approximations. Moreover, we use o_{ij} for the numerical approximation o_h in K_{ij} , and the cell average is \bar{o}_{ij} .

Let us consider how to construct positive u_h first, and the equation satisfied by the cell averages is

$$\bar{u}_{ij}^{n+1} = H_{ij}^c(u, r, s) + H_{ij}^d(u, p, q),$$

where

$$\begin{aligned} H_{ij}^c(u, r, s) &= \frac{1}{2} \bar{u}_{ij}^n - \frac{\Delta t}{\Delta x \Delta y} \left(\int_{J_j} (\widehat{ur}_{i+\frac{1}{2},j} - \widehat{ur}_{i-\frac{1}{2},j}) dy + \int_{I_i} (\widehat{us}_{i,j+\frac{1}{2}} - \widehat{us}_{i,j-\frac{1}{2}}) dx \right), \\ H_{ij}^d(u, p, q) &= \frac{1}{2} \bar{u}_{ij}^n + \frac{\Delta t}{\Delta x \Delta y} \left(\int_{J_j} (\hat{p}_{i+\frac{1}{2},j} - \hat{p}_{i-\frac{1}{2},j}) dy + \int_{I_i} (\hat{q}_{i,j+\frac{1}{2}} - \hat{q}_{i,j-\frac{1}{2}}) dx \right). \end{aligned}$$

For simplicity, if not otherwise stated, we will omit the subscript ij in H_{ij}^c and H_{ij}^d . To analyze H^c , we approximate the integral by a 2-point Gauss quadrature. The Gauss

quadrature points on I_i and J_j are denoted by

$$p_i^x = \{x_i^\beta : \beta = 1, 2\} \text{ and } p_j^y = \{y_j^\beta : \beta = 1, 2\},$$

respectively. Also, we denote w_β as the corresponding weights on the interval $[-\frac{1}{2}, \frac{1}{2}]$.

Let $\lambda_1 = \frac{\Delta t}{\Delta x}$ and $\lambda_2 = \frac{\Delta t}{\Delta y}$, then H^c becomes

$$H^c(u, r, s) = \frac{1}{2} \bar{u}_{ij}^n + \lambda_1 \sum_{\beta=1}^2 w_\beta \left(\widehat{ur}_{i-\frac{1}{2}, \beta} - \widehat{ur}_{i+\frac{1}{2}, \beta} \right) + \lambda_2 \sum_{\beta=1}^2 w_\beta \left(\widehat{us}_{\beta, j-\frac{1}{2}} - \widehat{us}_{\beta, j+\frac{1}{2}} \right),$$

where $\widehat{ur}_{i-\frac{1}{2}, \beta}$ is the numerical flux at $(x_{i-\frac{1}{2}}, y_j^\beta)$. Likewise for the other fluxes. As the general treatment, we rewrite the cell average on the right hand side as

$$\bar{u}_{ij}^n = \frac{1}{2} \sum_{\beta=1}^2 w_\beta \left(u_{i-\frac{1}{2}, \beta}^+ + u_{i+\frac{1}{2}, \beta}^- \right) = \frac{1}{2} \sum_{\beta=1}^2 w_\beta \left(u_{\beta, j-\frac{1}{2}}^+ + u_{\beta, j+\frac{1}{2}}^- \right),$$

where $u_{i-\frac{1}{2}, \beta}^- = u_{i-\frac{1}{2}, j}^-(y_j^\beta)$ is a point value of the numerical approximation in the Gauss quadrature. Likewise for the other point values. Define $\mu = \lambda_1 + \lambda_2$, then

$$\begin{aligned} H^c(u, r, s) &= \lambda_1 \sum_{\beta=1}^2 w_\beta \left[\frac{1}{4\mu} \left(u_{i-\frac{1}{2}, \beta}^+ + u_{i+\frac{1}{2}, \beta}^- \right) + \left(\widehat{ur}_{i-\frac{1}{2}, \beta} - \widehat{ur}_{i+\frac{1}{2}, \beta} \right) \right] \\ &\quad + \lambda_2 \sum_{\beta=1}^2 w_\beta \left[\frac{1}{4\mu} \left(u_{\beta, j-\frac{1}{2}}^+ + u_{\beta, j+\frac{1}{2}}^- \right) + \left(\widehat{us}_{\beta, j-\frac{1}{2}} - \widehat{us}_{\beta, j+\frac{1}{2}} \right) \right]. \end{aligned}$$

We need to suitably choose the parameter α in the Lax-Friedrichs flux, and the result is given below.

Lemma 4.1. *We can choose*

$$\alpha > \max_{\substack{1 \leq i \leq N_x - 1 \\ 1 \leq j \leq N_y - 1 \\ \beta = 1, 2}} \left\{ r_{i+\frac{1}{2}, \beta}^+, -r_{i+\frac{1}{2}, \beta}^-, s_{\beta, j+\frac{1}{2}}^+, -s_{\beta, j+\frac{1}{2}}^- \right\},$$

then $\bar{u}_j^{n+1} > 0$ under a CFL condition

$$A \left(\frac{\Delta t}{\Delta x} + \frac{\Delta t}{\Delta y} \right) \leq \frac{1}{2}, \quad (4.1)$$

where

$$A = \alpha - \min_{\substack{1 \leq i \leq N_x - 1 \\ 1 \leq j \leq N_y - 1 \\ \beta = 1, 2}} \left\{ r_{i+\frac{1}{2},\beta}^+, -r_{i+\frac{1}{2},\beta}^-, s_{\beta,j+\frac{1}{2}}^+, -s_{\beta,j+\frac{1}{2}}^- \right\} \geq 0,$$

Proof. It is easy to check, for $i = 2, 3, \dots, N_x$,

$$\begin{aligned} & \frac{1}{4\mu} u_{i-\frac{1}{2},\beta}^+ + \widehat{ur}_{i-\frac{1}{2},\beta} \\ &= \frac{1}{4\mu} u_{i-\frac{1}{2},\beta}^+ + \frac{1}{2} \left(u_{i-\frac{1}{2},\beta}^- r_{i-\frac{1}{2},\beta}^- + u_{i-\frac{1}{2},\beta}^+ r_{i-\frac{1}{2},\beta}^+ - \alpha (u_{i-\frac{1}{2},\beta}^+ - u_{i-\frac{1}{2},\beta}^-) \right) \\ &= \frac{1}{2} \left(\alpha + r_{i-\frac{1}{2},\beta}^- \right) u_{i-\frac{1}{2},\beta}^- + \frac{1}{2} \left(\frac{1}{2\mu} + r_{i-\frac{1}{2},\beta}^+ - \alpha \right) u_{i-\frac{1}{2},\beta}^+. \end{aligned}$$

Therefore, we can choose $\alpha + r_{i-\frac{1}{2},\beta}^- > 0$ and $\frac{1}{2\mu} + r_{i-\frac{1}{2},\beta}^+ - \alpha > 0$ to obtain $\frac{1}{4\mu} u_{i-\frac{1}{2},\beta}^+ + \widehat{ur}_{i-\frac{1}{2},\beta} > 0$. If $i = 1$, by (2.9),

$$\frac{1}{4\mu} u_{i-\frac{1}{2},\beta}^+ + \widehat{ur}_{i-\frac{1}{2},\beta} = \frac{1}{4\mu} u_{i-\frac{1}{2},\beta}^+ > 0.$$

Also, for $i = 1, 2, \dots, N_y - 1$,

$$\begin{aligned} & \frac{1}{4\mu} u_{i+\frac{1}{2},\beta}^- - \widehat{ur}_{i+\frac{1}{2},\beta} \\ &= \frac{1}{4\mu} u_{i+\frac{1}{2},\beta}^- - \frac{1}{2} \left(u_{i+\frac{1}{2},\beta}^- r_{i+\frac{1}{2},\beta}^- + u_{i+\frac{1}{2},\beta}^+ r_{i+\frac{1}{2},\beta}^+ - \alpha (u_{i+\frac{1}{2},\beta}^+ - u_{i+\frac{1}{2},\beta}^-) \right) \\ &= \frac{1}{2} \left(\alpha - r_{i+\frac{1}{2},\beta}^+ \right) u_{i+\frac{1}{2},\beta}^+ + \frac{1}{2} \left(\frac{1}{2\mu} - r_{i+\frac{1}{2},\beta}^- - \alpha \right) u_{i+\frac{1}{2},\beta}^-. \end{aligned}$$

We can choose $\alpha - r_{i+\frac{1}{2},\beta}^+ > 0$ and $\frac{1}{2\mu} - r_{i+\frac{1}{2},\beta}^- - \alpha > 0$ such that $\frac{1}{4\mu} u_{i+\frac{1}{2},\beta}^- - \widehat{ur}_{i+\frac{1}{2},\beta} > 0$. If $i = N_y$, then by (2.9),

$$\frac{1}{4\mu} u_{i+\frac{1}{2},\beta}^- - \widehat{ur}_{i+\frac{1}{2},\beta} = \frac{1}{4\mu} u_{i+\frac{1}{2},\beta}^- > 0.$$

Similarly, for $j = 2, 3, \dots, N_y$ we require $\alpha + s_{\beta,j-\frac{1}{2}}^- > 0$ and $\frac{1}{2\mu} + s_{\beta,j-\frac{1}{2}}^+ - \alpha > 0$ to obtain $\frac{1}{4\mu} u_{\beta,j-\frac{1}{2}}^+ + \widehat{us}_{\beta,j-\frac{1}{2}} > 0$. For $j = 1, 2, \dots, N_y - 1$, we need $\alpha - s_{\beta,j+\frac{1}{2}}^+ > 0$ and $\frac{1}{2\mu} - s_{\beta,j+\frac{1}{2}}^- - \alpha > 0$ such that $\frac{1}{4\mu} u_{\beta,j+\frac{1}{2}}^- - \widehat{us}_{\beta,j+\frac{1}{2}} > 0$. \square

Now, we proceed to analyze $H^d(p, q)$. Following the same analysis in [51] with some minor changes, we can show the following lemma.

Lemma 4.2. Suppose $u_{ij}^n > 0$ for all i and j , then

$$H^d(u, p, q) > 0$$

under a CFL condition

$$\frac{\Delta t}{\Delta x^2} + \frac{\Delta t}{\Delta y^2} \leq \frac{1}{20}. \quad (4.2)$$

Proof. Define $H^d(u, p, q) = \frac{1}{\Delta y} H^1(u, p) + \frac{1}{\Delta x} H^2(u, q)$, where

$$H_1^d(u, p) = \int_{J_j} \left[\frac{\Lambda_1}{4\Lambda} \left(u_{i-\frac{1}{2},j}^+ + u_{i+\frac{1}{2},j}^- \right) - \lambda_1 \left(\widehat{p}_{i-\frac{1}{2},j} - \widehat{p}_{i+\frac{1}{2},j} \right) \right] dy \quad (4.3)$$

$$H_2^d(u, q) = \int_{I_i} \left[\frac{\Lambda_2}{4\Lambda} \left(u_{i,j-\frac{1}{2}}^+ + u_{i,j+\frac{1}{2}}^- \right) - \lambda_2 \left(\widehat{q}_{i,j-\frac{1}{2}} - \widehat{q}_{i,j+\frac{1}{2}} \right) \right] dx, \quad (4.4)$$

with $\Lambda_1 = \frac{\Delta t}{\Delta x^2}$, $\Lambda_2 = \frac{\Delta t}{\Delta y^2}$ and $\Lambda = \Lambda_1 + \Lambda_2$. It is easy to check that

$$\begin{aligned} \int_{J_j} p_{i+\frac{1}{2},j}^- dy &= \int_{J_j} \frac{1}{\Delta x} \left(4u_{i+\frac{1}{2},j}^+ - 3u_{i+\frac{1}{2},j}^- - u_{i-\frac{1}{2},j}^+ \right) dy, \quad i = 1, \dots, N_x - 1, \\ \int_{I_i} q_{i,j+\frac{1}{2}}^- dx &= \int_{I_i} \frac{1}{\Delta y} \left(4u_{i,j+\frac{1}{2}}^+ - 3u_{i,j+\frac{1}{2}}^- - u_{i,j-\frac{1}{2}}^+ \right) dx, \quad j = 1, \dots, N_y - 1. \end{aligned}$$

Plug the flux (2.5) into (4.3) to obtain

1. $i = 1$

$$\begin{aligned} &H_1^d(u, p) \\ &= \int_{J_j} \left[\frac{\Lambda_1}{4\Lambda} u_{i+\frac{1}{2},j}^- + \frac{\Lambda_1}{4\Lambda} u_{i-\frac{1}{2},j}^+ + \lambda_1 p_{i+\frac{1}{2},j}^- \right] dy \\ &= \int_{J_j} \left[\left(\frac{\Lambda_1}{4\Lambda} - \Lambda_1 \right) u_{i-\frac{1}{2},j}^+ + \left(\frac{\Lambda_1}{4\Lambda} - 3\Lambda_1 \right) u_{i+\frac{1}{2},j}^- + 4\Lambda_1 u_{i+\frac{1}{2},j}^+ \right] dy \\ &> 0. \end{aligned}$$

2. $2 \leq i \leq N_x - 1$

$$\begin{aligned} &H_1^d(u, p) \\ &= \int_{J_j} \left[\frac{\Lambda_1}{4\Lambda} u_{i+\frac{1}{2},j}^- + \frac{\Lambda_1}{4\Lambda} u_{i-\frac{1}{2},j}^+ + \lambda_1 \left(p_{i+\frac{1}{2},j}^- - p_{i-\frac{1}{2},j}^- \right) \right] dy \\ &= \int_{J_j} \left[\Lambda_1 u_{i-\frac{3}{2},j}^+ + 3\Lambda_1 u_{i-\frac{1}{2},j}^- + \left(\frac{\Lambda_1}{4\Lambda} - 5\Lambda_1 \right) u_{i-\frac{1}{2},j}^+ + \left(\frac{\Lambda_1}{4\Lambda} - 3\Lambda_1 \right) u_{i+\frac{1}{2},j}^- + 4\Lambda_1 u_{i+\frac{1}{2},j}^+ \right] dy \\ &> 0. \end{aligned}$$

3. $i = N_x$

$$\begin{aligned}
& H_1^d(u, p) \\
&= \int_{J_j} \left[\frac{\Lambda_1}{4\Lambda} u_{i+\frac{1}{2},j}^- + \frac{\Lambda_1}{4\Lambda} u_{i-\frac{1}{2},j}^+ - \lambda_1 p_{i-\frac{1}{2},j}^- \right] dy \\
&= \int_{J_j} \left[\Lambda_1 u_{i-\frac{3}{2},j}^+ + 3\Lambda_1 u_{i-\frac{1}{2},j}^- + \left(\frac{\Lambda_1}{4\Lambda} - 4\Lambda_1 \right) u_{i-\frac{1}{2},j}^+ + \frac{\Lambda_1}{4\Lambda} u_{i+\frac{1}{2},j}^- \right] dy \\
&> 0.
\end{aligned}$$

We can analyze H_2^d in a similar way, so we skip the proof. □

Based on the above two lemmas, we have the following theorem.

Theorem 4.1. *Suppose $u_{ij}^n > 0$ for all i and j , then*

$$\bar{u}_{ij}^{n+1} > 0$$

under the CFL conditions (4.1) and (4.2).

Now, let us proceed to analyze v , and the equation satisfied by the numerical cell averages is

$$\begin{aligned}
\bar{v}_{ij}^{n+1} &= \frac{1}{2} \bar{v}_{ij}^n + H^d(v, r, s) + \Delta t (\bar{u}_{ij}^n - \bar{v}_{ij}^n) \\
&= H^d(v, r, s) + \left(\frac{1}{2} - \Delta t \right) \bar{v}_{ij}^n + \Delta t \bar{u}_{ij}^n.
\end{aligned}$$

Applying Lemma 4.2, it is easy to prove the following theorem.

Theorem 4.2. *Suppose $v_{ij}^n > 0$ for all i and j , then*

$$\bar{v}_{ij}^{n+1} > 0$$

provided

$$\frac{\Delta t}{\Delta x^2} + \frac{\Delta t}{\Delta y^2} \leq \frac{1}{20},$$

and

$$\Delta t \leq \frac{1}{2}.$$

Based on Theorems 4.1 and 4.2, the numerical cell averages we obtained are positive. However, the numerical solutions u_{ij}^n and v_{ij}^n might still be negative. Hence, we have to modify the numerical solutions while keeping the cell averages untouched. For simplicity, we discuss the modification of u_{ij}^n only and the procedure is given in the following steps.

- Set up a small number $\varepsilon = 10^{-13}$.
- If $\bar{u}_{ij}^n > \varepsilon$, then proceed to the following steps. Otherwise, u_{ij}^n is identified as the approximation to vacuum, and we will take $\tilde{u}_{ij}^n = \bar{u}_{ij}^n$ as the numerical solution and skip the following steps.
- Modify the density: Compute

$$b_{ij} = \min_{(x,y) \in K_{ij}} u_{ij}^n(x, y).$$

If $b_{ij} < \varepsilon$, then take \tilde{u}_{ij}^n as

$$\tilde{u}_{ij}^n = \bar{u}_{ij}^n + \theta_{ij} (u_{ij}^n - \bar{u}_{ij}^n),$$

with

$$\theta_{ij} = \frac{\bar{u}_{ij}^n - \varepsilon}{\bar{u}_{ij}^n - b_{ij}},$$

and use \tilde{u}_{ij}^n as the new numerical density u_{ij}^n .

Remark 4.1. In the third step mentioned above, the limiter does not change the numerical cell averages. Actually, since

$$\frac{1}{\Delta x \Delta y} \int_{K_{ij}} u_{ij}^n = \bar{u}_{ij}^n,$$

then we have

$$\frac{1}{\Delta x \Delta y} \int_{K_{ij}} \tilde{u}_{ij}^n = \bar{u}_{ij}^n + \theta_{ij} \left(\frac{1}{\Delta x \Delta y} \int_{K_{ij}} u_{ij}^n - \bar{u}_{ij}^n \right) = \bar{u}_{ij}^n.$$

Following [34, 45], we can show the L^1 -stability of the numerical scheme with the positivity-preserving limiter. Since u_h^n is positive, we have

$$\|u_h^n\|_{L^1} = \int_{\Omega} u_h^n(x) dx = \int_{\Omega} u_h^0(x) dx = \|u_h^0\|_{L^1},$$

where $\|u\|_{L^1}$ is the standard L^1 -norm of u on Ω . This implies the L^1 -stability of the scheme.

Remark 4.2. The positivity preserving limiter mentioned above does not kill the accuracy which was proved in [49, 50].

4.1 High order time discretizations

All the previous analyses are based on first-order Euler forward time discretization. We can also use strong stability preserving (SSP) high-order time discretizations to solve the ODE system $\mathbf{w}_t = \mathbf{L}\mathbf{w}$. More details of these time discretizations can be found in [39, 38, 19]. In this paper, we use the third order SSP Runge-Kutta method [39]

$$\begin{aligned}\mathbf{w}^{(1)} &= \mathbf{w}^n + \tau\mathbf{L}(\mathbf{w}^n), \\ \mathbf{w}^{(2)} &= \frac{3}{4}\mathbf{w}^n + \frac{1}{4}(\mathbf{w}^{(1)} + \tau\mathbf{L}(\mathbf{w}^{(1)})), \\ \mathbf{w}^{n+1} &= \frac{1}{3}\mathbf{w}^n + \frac{2}{3}(\mathbf{w}^{(2)} + \tau\mathbf{L}(\mathbf{w}^{(2)})),\end{aligned}\tag{4.5}$$

with time step $\tau \leq \Delta t$ where Δt was given in Theorem 4.2 and the third order SSP multi-step method [38]

$$\mathbf{w}^{n+1} = \frac{16}{27}(\mathbf{w}^n + 3\tau\mathbf{L}(\mathbf{w}^n)) + \frac{11}{27}\left(\mathbf{w}^{n-3} + \frac{12}{11}\tau\mathbf{L}(\mathbf{w}^{n-3})\right).\tag{4.6}$$

with time step $\tau \leq \frac{1}{3}\Delta t$. Since an SSP time discretization is a convex combination of Euler forward, by using the limiter mentioned in Section 4, the numerical solutions obtained from the full scheme are also positive.

5 Numerical experiments

In this section, we present numerical examples in two space dimensions to verify the theoretical analysis and the positivity-preserving property of the proposed method. If not otherwise stated, we use P^1 -LDG method with third-order Runge-Kutta time discretization.

Example 5.1. We solve the following problem on the domain $\Omega = [0, 2\pi] \times [0, 2\pi]$

$$\begin{aligned}u_t - \operatorname{div}(\nabla u - u\nabla v) &= 0, & x \in \Omega, t > 0 \\ v_t - \Delta v &= u - v, & x \in \Omega, t > 0,\end{aligned}\tag{5.1}$$

We use spectral method with enough points to compute a reference solution at $t = 0.2$, which can be considered as the exact solution. In Table 5.1, we present the numerical results for the proposed method with and without the bound preserving limiters. From the table, we can observe optimal rate of convergence with V_h^1 finite element spaces.

N	no limiter		with limiter	
	L^2 error	order	L^2 error	order
20	9.25e-3	–	1.16e-2	–
40	2.34e-3	1.98	2.40e-3	2.27
80	5.82e-4	2.01	5.84e-4	2.04
160	1.45e-4	2.00	1.45e-4	2.01

Table 5.1: Example 5.1: accuracy test at $T = 0.2$ for the second-order LDG methods with and without the positivity-preserving limiter. $N_x = N_y = N$.

Example 5.2. In this example, we solve (1.1) with the following initial condition.

$$u_0 = 840 \exp(-84(x^2 + y^2)), \quad v_0 = 420 \exp(-42(x^2 + y^2)).$$

We use second-order positivity-preserving LDG methods and the numerical approximations at time t are given in Figure 5.1. In [15], the authors demonstrated that the blow-up time

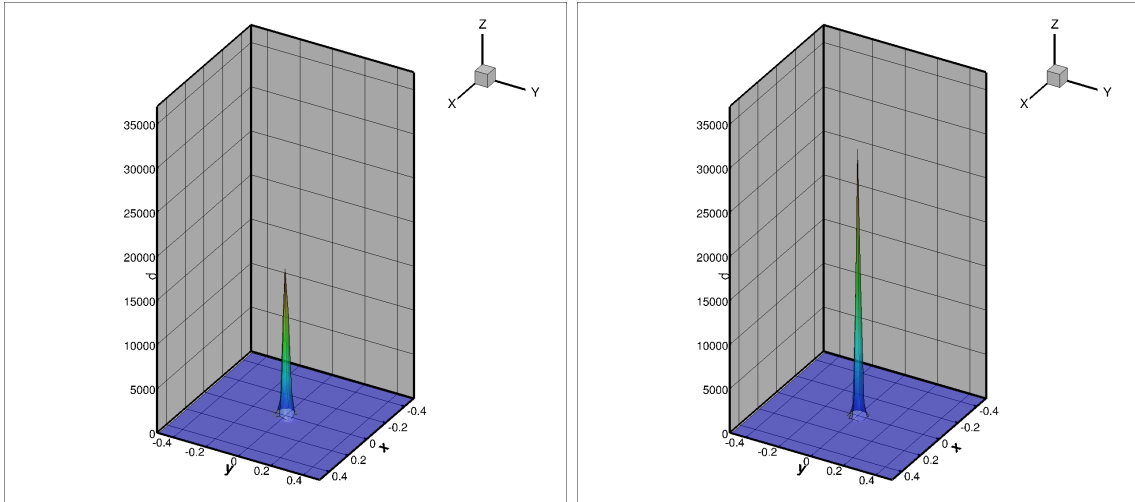


Figure 5.1: Example 5.2: Numerical approximations of u at $t = 6 \times 10^{-5}$ (left) and $t = 1.2 \times 10^{-4}$ with positivity-preserving limiter for P^1 polynomials and $N = 160$.

should be approximately $t = 1.21 \times 10^{-4}$. However, we can continue our numerical simulation

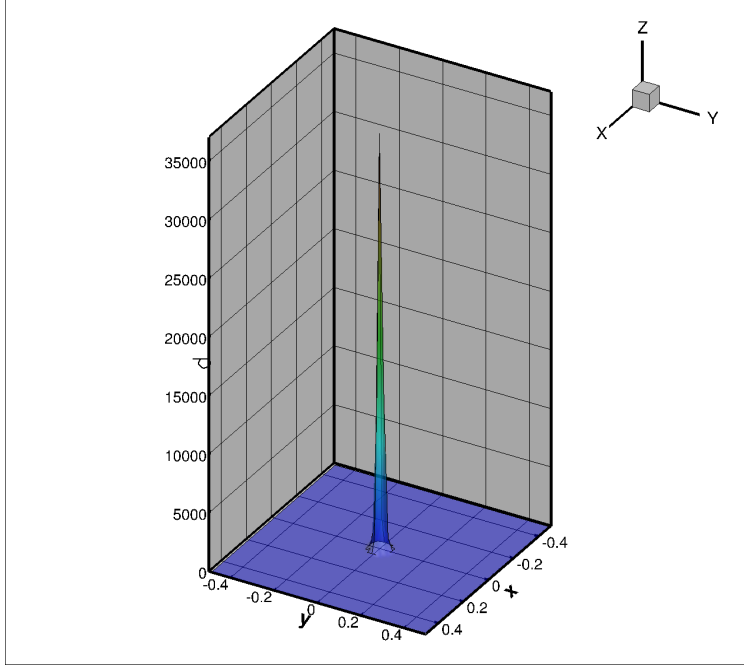


Figure 5.2: Example 5.2: Numerical approximations of u at $t = 2.0 \times 10^{-4}$ with positivity-preserving limiter for P^1 polynomials and $N = 160$.

to $t = 2 \times 10^{-4}$, and the numerical approximation is given in figure 5.2. We also solve the problem without the positivity-preserving limiter. We find that at about $t = 8 \times 10^{-5}$ the numerical scheme yields negative u .

Moreover, we also test the numerical blow-up time. For simplicity, we take $N_x = N_y = N$, and compute the L^2 -norm numerical approximations at time t with $N \times N$ cells, defined as $S(N, t)$. Define

$$t_b(N) = \inf\{t : S(2N, t) * 1.05\% \geq S(N, t)\} \quad (5.2)$$

as the numerical blow-up time. We anticipate that as we refine the mesh, the numerical blow-up time will converge to the exact value. However, due to the computational cost, we have to apply adaptive methods and refine the mesh in the vicinity of the blow-up point, and this work will be considered in the future. To verify our anticipation, we consider the following function

$$f(x, t) = \frac{1}{1-t} \exp\left(\frac{-x^2}{2(t-1)^2}\right). \quad (5.3)$$

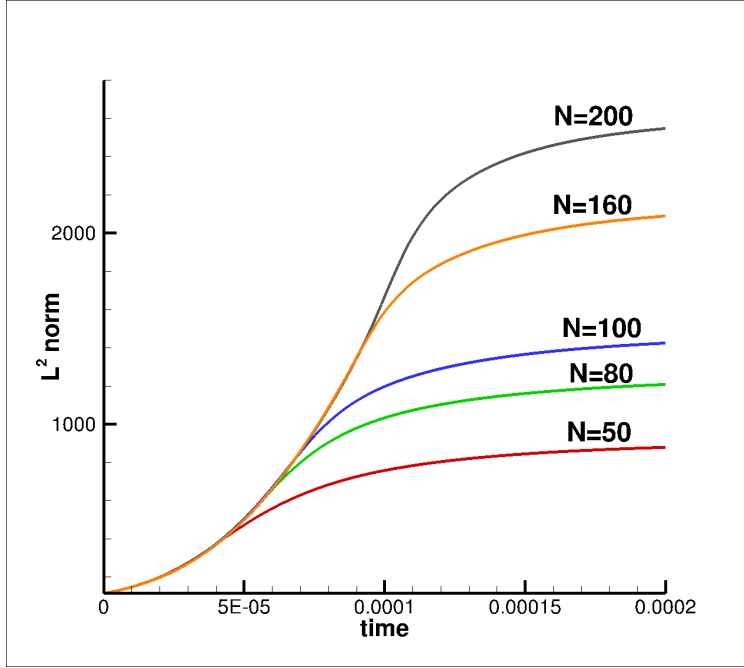


Figure 5.3: L^2 -norm of the numerical approximation for Example 5.2 with different N 's.

It is easy to see that

$$\lim_{t \rightarrow 1^-} f(x, t) \rightarrow \delta(x)$$

in the sense of distribution.

We consider the interval $[-1,1]$ and divided in into N uniform cells. Denote u_h , the L^2 -projection of $f(x, t)$, as the numerical approximation in each cell and $S(N, t)$ to be the L^2 -norm of u_h over $[-1,1]$ with different t 's. We also compute the numerical blow-up time $t_b(N)$ by (5.2) and the results are given in Table 5.2. We can clearly see that as we refine the meshes, $t_b(N)$ converges to 1, the exact blow-up time, in first order accuracy.

N	10	20	40	80	160	320
Blow-up time	-	0.671	0.836	0.918	0.959	0.980
Error	-	0.329	0.164	0.092	0.041	0.020

Table 5.2: Numerical blow-up time with different mesh sizes for (5.3).

6 Conclusion

In this paper, we develop LDG methods to the KS chemotaxis model. We improve the result given by [15], and give the optimal error estimate under special finite element spaces. A special positivity-preserving limiter is constructed to obtain physically relevant numerical approximations. Moreover, we also prove the L^1 -stability of the LDG scheme with the limiter. Numerical experiments are given to demonstrate the good performance of the LDG scheme and the estimate of the numerical blow-up time. In the future, we plan to apply adaptive methods to calculate the blow-up time more accurately.

7 Acknowledgments

Xingjie Helen Li would like to thank the Shanghai Centre for Mathematics Science (SCMS), Fudan University, for support during her visit.

References

- [1] F. Bassi and S. Rebay, *A high-order accurate discontinuous finite element method for the numerical solution of the compressible Navier-Stokes equations*, Journal of Computational Physics, 131 (1997), 267-279.
- [2] A. Chertock and A. Kurganov, *A second-order positivity preserving central-upwind scheme for chemotaxis and haptotaxis models*, Numerische Mathematik, 111 (2008), 169-205.
- [3] S. Childress and J. Percus, *Nonlinear aspects of chemotaxis*, Mathematical Biosciences, 56 (1981), 217-237.
- [4] P. Ciarlet, *Finite Element Method for Elliptic Problems*, North-Holland, Amsterdam, 1978.

- [5] B. Cockburn and B. Dong, *An analysis of the minimal dissipation local discontinuous Galerkin method for convection-diffusion problems*, Journal of Scientific Computing, 32 (2007), 233-262.
- [6] B. Cockburn, S. Hou and C.-W. Shu, *The Runge-Kutta local projection discontinuous Galerkin finite element method for conservation laws IV: the multidimensional case*, Mathematics of Computation, 54 (1990), 545-581.
- [7] B. Cockburn, G. Kanschat, I. Perugia, and D. Schotzau, *Superconvergence of the local discontinuous Galerkin method for elliptic problems on cartesian grids*, SIAM Journal on Numerical Analysis, 39 (2001), 264-285.
- [8] B. Cockburn, S.-Y. Lin and C.-W. Shu, *TVB Runge-Kutta local projection discontinuous Galerkin finite element method for conservation laws III: one-dimensional systems*, Journal of Computational Physics, 84 (1989), 90-113.
- [9] B. Cockburn and C.-W. Shu, *TVB Runge-Kutta local projection discontinuous Galerkin finite element method for conservation laws II: general framework*, Mathematics of Computation, 52 (1989), 411-435.
- [10] B. Cockburn and C.-W. Shu, *The Runge-Kutta discontinuous Galerkin method for conservation laws V: multidimensional systems*, Journal of Computational Physics, 141 (1998), 199-224.
- [11] B. Cockburn and C.-W. Shu, *The local discontinuous Galerkin method for time dependent convection-diffusion systems*, SIAM Journal on Numerical Analysis, 35 (1998), 2440-2463.
- [12] Y. Epshteyn, *Discontinuous Galerkin methods for the chemotaxis and haptotaxis models*, Journal of Computational and Applied Mathematics, 224 (2009), 168-181.

- [13] Y. Epshteyn, *Upwind-difference potentials method for Patlak-Keller-Segel chemotaxis model*, Journal of Scientific Computing, 53 (2012), 689-713.
- [14] Y. Epshteyn and A. Izmirliglu, *Fully discrete analysis of a discontinuous finite element method for the Keller-Segel Chemotaxis model*, Journal of Scientific Computing, 40 (2009), 211-256.
- [15] Y. Epshteyn and A. Kurganov, *New interior penalty discontinuous Galerkin methods for the Keller-Segel Chemotaxis model*, SIAM Journal on Numerical Analysis, 47 (2008), 368-408.
- [16] F. Filbet, *A finite volume scheme for the Patlak-Keller-Segel chemotaxis model*, Numerische Mathematik, 104 (2006), 457-488.
- [17] H. Gajewski and K. Zacharias, *Global behaviour of a reaction-diffusion system modelling chemotaxis*, Mathematische Nachrichten, 195 (1998), 77-114.
- [18] I.M. Gelfand, *Some questions of analysis and differential equations*, American Mathematical Society Translations, 26 (1963), 201-219.
- [19] S. Gottlieb, C.-W. Shu and E. Tadmor, *Strong stability-preserving high-order time discretization methods*, SIAM Review, 43 (2001), 89-112.
- [20] L. Guo and Y. Yang, *Positivity-preserving high-order local discontinuous Galerkin method for parabolic equations with blow-up solutions*, Journal of Computational Physics, 289 (2015), 181-195.
- [21] I. Fatkullin, *A study of blow-ups in the Keller-Segel model of chemotaxis*, Nonlinearity, 26 (2013), 81-94.
- [22] J. Hakovec and C. Schmeiser, *Stochastic particle approximation for measure valued solutions of the 2d Keller-Segel system*, Journal of Statistical Physics, 135 (2009), 133-151.

- [23] M.A. Herrero, E. Medina and J.J.L. Velázquez, *Finite-time aggregation into a single point in a reaction-diffusion system*, Nonlinearity, 10 (1997), 1739-1754.
- [24] M. A. Herrero, J.J. L. Velazquez, *Singularity patterns in a chemotaxis model*, Mathematics Annuals, 306 (1996), 583-623.
- [25] D. Horstman, *From 1970 until now: The Keller-Segel model in chemotaxis and its consequences I*, Jahresbericht DMV, 105 (2003), 103-165.
- [26] D. Horstmann, *From 1970 until now: The Keller-Segel model in chemotaxis and its consequences II*, Jahresbericht DMV, 106 (2004), 51-69.
- [27] A.E. Hurd and D.H. Sattinger, *Questions of existence and uniqueness for hyperbolic equations with discontinuous coefficients*, Transactions of the American Mathematical Society, 132 (1968), 159-174.
- [28] E.F. Keller and L.A. Segel, *Initiation on slime mold aggregation viewed as instability*, Journal of Theoretical Biology, 26 (1970), 399-415.
- [29] A. Marrocco, *2D simulation of chemotaxis bacteria aggregation*, ESAIM: Mathematical Modelling and Numerical Analysis (M^2AN), 37 (2003), 617-630.
- [30] X. Meng, C.-W. Shu, Q. Zhang and B. Wu, *Superconvergence of discontinuous Galerkin methods for scalar nonlinear conservation laws in one space dimension*, SIAM Journal on Numerical Analysis, 50 (2012), 2336-2356.
- [31] T. Nagai, *blow-up of radially symmetric solutions to a chemotaxis system*, Advances in Mathematical Sciences and Applications, 3 (1995), 581-601.
- [32] E. Nakaguchi and Y. Yagi, *Fully discrete approximation by Galerkin Runge-Kutta methods for quasilinear parabolic systems*, Hokkaido Mathematical Journal, 31 (2002), 385-429.

- [33] C. Patlak, *Random walk with persistence and external bias*, The Bulletin of Mathematical Biophysics, 15 (1953), 311-338.
- [34] T. Qin, C.-W. Shu and Y. Yang, *Bound-preserving discontinuous Galerkin methods for relativistic hydrodynamics*, Journal of Computational Physics, 315 (2016), 323-347.
- [35] W.H. Reed and T.R. Hill, *Triangular mesh methods for the Neutron transport equation*, Los Alamos Scientific Laboratory Report LA-UR-73-479, Los Alamos, NM, 1973.
- [36] N. Saito, *Conservative upwind finite-element method for a simplified Keller-Segel system modelling chemotaxis*, IMA Journal of Numerical Analysis, 27 (2007), 332-365.
- [37] N. Saito, *Error analysis of a conservative finite-element approximation for the Keller-Segel system of chemotaxis*, Communications on Pure and Applied Analysis, 11 (2012), 339-364.
- [38] C.-W. Shu, *Total-variation-diminishing time discretizations*, SIAM Journal on Scientific and Statistical Computing, 9 (1988), 1073-1084.
- [39] C.-W. Shu and S. Osher, *Efficient implementation of essentially non-oscillatory shock-capturing schemes*, Journal of Computational Physics, 77 (1988), 439-471.
- [40] R. Strehl, A. Sokolov, D. Kuzmin, D. Horstmann, and S. Turek, *A positivity-preserving finite element method for chemotaxis problems in 3D*, Journal of Computational and Applied Mathematics, 239 (2013), 290-303.
- [41] R. Tyson, L.J. Stern and R.J. LeVeque, *Fractional step methods applied to a chemotaxis model*, Journal of Mathematical Biology, 41 (2000), 455-475.
- [42] H. Wang, C.-W. Shu and Q. Zhang, *Stability and error estimates of local discontinuous Galerkin methods with implicit-explicit time-marching for advection-diffusion problems*, SIAM Journal on Numerical Analysis, 53 (2015), 206-227.

- [43] H. Wang, S. Wang, C.-W. Shu and Q. Zhang, *Local discontinuous Galerkin methods with implicit-explicit time-marching for multi-dimensional convection-diffusion problems*, ESAIM: Mathematical Modelling and Numerical Analysis (M^2AN), to appear. DOI: <http://dx.doi.org/10.1051/m2an/2015068>
- [44] Y. Yang and C.-W. Shu, *Discontinuous Galerkin method for hyperbolic equations involving δ -singularities: negative-order norm error estimates and applications*, Numerische Mathematik, 124, (2013), 753-781.
- [45] Y. Yang, D. Wei and C.-W. Shu, *Discontinuous Galerkin method for Krause's consensus models and pressureless Euler equations*, Journal of Computational Physics, 252 (2013), 109-127.
- [46] Q. Zhang and C.-W. Shu, *Error estimates to smooth solutions of Runge-Kutta discontinuous Galerkin methods for scalar conservation laws*, SIAM Journal on Numerical Analysis, 42 (2004), 641-666.
- [47] Q. Zhang and C.-W. Shu, *Stability analysis and a priori error estimates to the third order explicit Runge-Kutta discontinuous Galerkin method for scalar conservation laws*, SIAM Journal on Numerical Analysis, 48 (2010), 1038-1063.
- [48] X. Zhang and C.-W. Shu, *On maximum-principle-satisfying high order schemes for scalar conservation laws*, Journal of Computational Physics, 229 (2010), 3091-3120.
- [49] X. Zhang and C.-W. Shu, *On positivity preserving high order discontinuous Galerkin schemes for compressible Euler equations on rectangular meshes*, Journal of Computational Physics, 229 (2010), 8918-8934.
- [50] X. Zhang and C.-W. Shu, *Positivity-preserving high order discontinuous Galerkin schemes for compressible Euler equations with source terms*, Journal of Computational Physics, 230 (2011), 1238-1248.

- [51] Y. Zhang, X. Zhang and C.-W. Shu, *Maximum-principle-satisfying second order discontinuous Galerkin schemes for convection-diffusion equations on triangular meshes*, Journal of Computational Physics, 234 (2013), 295-316.
- [52] X. Zhao, Y. Yang and C. Syler, *A positivity-preserving semi-implicit discontinuous Galerkin scheme for solving extended magnetohydrodynamics equations*, Journal of Computational Physics, 278 (2014), 400-415.